ACS APPLIED MATERIALS & INTERFACES

Research Article

www.acsami.org

Selective Detection of Iodide and Cyanide Anions Using Gold-Nanoparticle-Based Fluorescent Probes

Shih-Chun Wei,[†] Pang-Hung Hsu,[†,‡] Yen-Fei Lee,[†] Yang-Wei Lin,*[,§] and Chih-Ching Huang*[,†,‡]

[†]Institute of Bioscience and Biotechnology and [‡]Center for Marine Bioenvironment and Biotechnology (CMBB), National Taiwan Ocean University, 2 Beining Road, Keelung 20224, Taiwan

[§]Department of Chemistry, National Changhua University of Education, No. 1 Jin-De Road, Changhua City 500, Taiwan

Supporting Information

ABSTRACT: We developed two simple, rapid, and cost-effective fluorescent nanosensors, both featuring bovine serum albumin labeled with fluorescein isothiocyanate (FITC))-capped gold nanoparticles (FITC−BSA−Au NPs), for the selective sensing of cyanide (CN^-) and iodine (I^-) ions in high-salinity solutions and edible salt samples. During the preparation of FITC−BSA−Au NP probes, when AuNPs were introduced to the mixture containing FITC and BSA, the unconjugated FITC and FITC-labeled BSA (FITC−BSA) adsorbed to the particles' surfaces. These probes operated on a basic principle that I^- and CN^- deposited on the surfaces of the Au NPs or the etching of Au NPs induced the release of FITC molecules or FITC−BSA into the solution, and thus restored the florescence of FITC. We employed FITC−BSA to protect the Au NPs from significant aggregation in high-salinity solutions. In the presence of masking agents such as $S_2O_8^{2-}/Pb^{2+}$, FITC−BSA−Au NPs facilitated the selective detection of CN^- (by at least 150-fold in comparison with other anions). We also demonstrated that the FITC−BSA−Au NPs in the presence of H_2O_2 could selectively detect I^- down to 50 nM. Taking advantages of their high stability and selectivity, we employed our FITC−BSA−Au NP-based probes for the detection of CN^- and I^- in water samples (pond water, tap water, and seawater) and detection of I^- in edible salt samples, respectively. This simple, rapid, and cost-effective sensing system appears to demonstrate immense practical potential for the detection of anions in real samples.

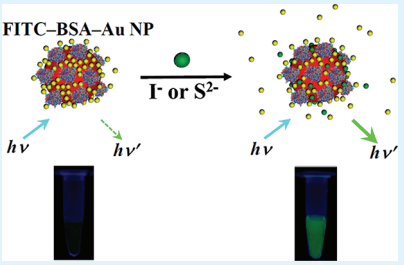

KEYWORDS: *cyanide, iodide, gold nanoparticles, fluorescence detection, edible salt*

INTRODUCTION

Gold nanoparticles (Au NPs) are the most commonly used optical sensing nanomaterials because of their high extinction coefficients and distance-dependent optical properties in the visible region.[1,2] In addition, the surface of Au NPs is versatile and it can be easily modified with various biofunctional groups (e.g., amphiphilic polymers, silanols, sugars, nucleic acids, proteins) through strong covalent bonding or physical adsorption.[3−5] As a result, many Au-NP-based colorimetric and fluorescent sensors were developed to detect metal ions, proteins, small molecules, DNA, pathogens, cells, and biocatalysts.[6−8] However, preparation of fluorophore conjugated Au NP probes usually involves tedious processes for labeling the probes and/or target analytes and use expensive fluorophores and coupling reagents.[9−12] Thus, label-free Au-NP nanosensors are in high demand for the trace analysis of small molecules and biomacromolecules.

The selective sensing of important anions, such as halide (Cl^-, Br^-, and I^-), sulfide (S^{2-}), and cyanide (CN^-) ions are highly significant because they are widely distributed and play important roles in both environmental and life sciences.[13−20] For example, iodide (I^-) is used to produce thyroid hormones such as triiodothyronine (T3) and thyroxine (T4) in the thyroid gland, which control many metabolic activities in the human body.[13] In addition, two thyroid proteins sodium/iodide symporter and iodotyrosine deiodinase are primarily responsible for the efficient utilization of dietary iodide in mammals.[14] Notably, deficiencies in either dietary iodide (recommended daily allowance of 150 μg/day) or in the metabolism of iodide may lead to goiter, hypothyroidism, and hyperthyroidism, and in severe cases it may produce developmental defects.[15] However, iodide quite rarely exists in the environment, and even seawater contains a very low iodide concentration (<1 μM), which is much lower than those of F^-, Cl^-, and Br^-.[16,17] Cyanide is an extremely lethal poison because of its propensity to bind to the active site of cytochrome oxidase, which eventually inhibits the electron transport in mitochondria.[17,18] The exposure to higher concentrations of CN^- (>300 ppm) within few minutes will cause human death by depressing the central nervous system.[19,20] Since it is lethal to humans and aquatic life, the U.S. Environmental Protection Agency (EPA) regulates the levels of cyanide that are allowable as 200 and 5 ppb for drinking water and environmental primary standards, respectively.[21]

To date, many strategies have been proposed for the detection of I^- and CN^- in aqueous solutions, including liquid

Received: February 21, 2012
Accepted: April 23, 2012
Published: April 23, 2012

   dx.doi.org/10.1021/am3003044 | ACS Appl. Mater. Interfaces 2012, 4, 2652−2658

chromatography–mass spectrometry (MS); liquid chromatography–atomic emission spectrometry (AES); capillary electrophoresis coupled with absorption or fluorescence detection; and electrochemical techniques.[22−27] However, these techniques are rather time-consuming, involve tedious sample preparations, and specific operating skills are indispensable. Moreover, the performance of some techniques have been seriously influenced by the interference of coexisting anions, while more complex and expensive instruments are mandatory for others. Recently, some chromogenic and fluorogenic chemosensors were developed to sense I^- and CN^-.[28−34] For example, a series of vitamin B_{12} derivatives can identify cyanide by colorimetric sensing based on displacement reactions.[34] Nevertheless, such chemosensors also suffer from some disadvantages, such as complicated organic synthesis, environmentally harmful systems, water insolubility, poor photostability, high detection limits, or easy interference from other anions. From the viewpoint of practical applications, an excellent sensor should be not only highly sensitive and selective but also simple and economical to operate. Thus, the development of new, practical optical assays for I^- and CN^- remains a challenge.

Recently, the unique optical properties of Au NPs have received considerable attention and thus they have been employed for the detection of I^-, CN^-, S^{2-}, nitrite, nitrate, phosphate, and thiocyanate.[35−54] For example, colorimetric probes that control the stability (aggregation) of Au NPs after the adsorption of I^- or CN^- on the surface of particles have been reported.[37,39] CN^- and I^- induced the displacement and/or dissolution of organic-dye-adsorbed Au NPs, which allowed the fluorescent turn-on detection of I^- and CN^-.[36,40−42] A label-free, Au-NP-based, surface-enhanced Raman scattering (SERS) probe for the direct sensing of CN^-, I^-, and SCN^- via the measurement of the Raman signals of anions after their deposition on Au NPs have also been reported.[39,41] Recently, Yang et al. reported a novel colorimetric probe for the detection of I^- using simple citrate-stabilized core–shell Cu@Au NPs through the I^--induced transformation of original nonspherical clusters to large, single, spherical ones.[38] This concept was further extended to sensing S^{2-} and cysteine by the competitive interaction of S^{2-}/cysteine and I^- toward Cu@Au NPs.[51] More recently, fluorescent, BSA-stabilized Au nanoclusters (NCs) and DNA-templated Au/Ag NC probes were used for the detection of CN^- and S^{2-} in a turn-off manner, respectively.[46,47] Although these methods provide greater affordability and portability to anion detection, few of them can be applied to high-salinity environmental matrices. In addition, selectivity is still a problem, because most of these probes are based on strong interactions between Au^+ and these anions (CN^-, I^-, and S^{2-}) at the particles' surfaces.

In this study, we developed a Au-NP-based fluorescent sensor for the selective detection of I^- and CN^- anions in aqueous solution. By introducing Au NPs to a mixed solution of fluorescein isothiocyanate (FITC) and bovine serum albumin (BSA), the unconjugated FITC and FITC-labeled BSA (FITC–BSA) will adsorb to the particles' surfaces during the preparation of FITC–BSA–Au NP probes. We employed FITC–BSA to protect the Au NPs from significant aggregation in high-salinity solutions. This probe operated on a basic principle that CN^-, I^-, and S^{2-} deposited on the surfaces of the Au NPs or the etching of Au NPs induced the release of FITC molecules or FITC–BSA into the solution, and thus restored the florescence of FITC (see Scheme 1). In the presence of the masking reagents such as thiosulfate pentahydrate ($S_2O_8^{2-}$)/Pb^{2+} ions and H_2O_2, our FITC–BSA–Au NP sensor is capable of detecting trace levels of I^- and CN^-, respectively. We have also demonstrated the practical feasibility of this approach for the analysis of I^- and CN^- ions in pond water, tap water, and high-salinity seawater samples. In addition, the H_2O_2–FITC–BSA–Au NP-based assay facilitate a simple, rapid, and accurate analysis of I^- levels in edible salts.

Scheme 1. Cartoon Representation of the Preparation of the FITC–BSA–Au NPs Fluorescent Sensor for the Detection of Anions Based on the Displacement of FITC Units on Au NPs or Dissolution of Au NPs

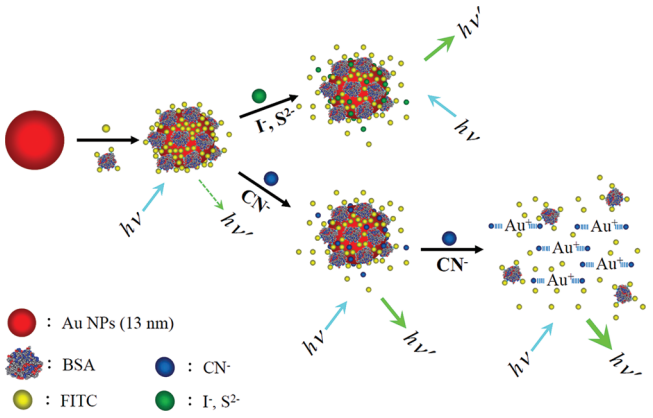

EXPERIMENTAL SECTION

Chemicals. FITC, BSA, trisodium citrate, H_3PO_4, Na_3PO_4, and $Pb(NO_3)_2$ used in this study were purchased from Aldrich (Milwaukee, WI). Hydrogen tetrachloroaurate(III) trihydrate, sodium thiosulfate pentahydrate ($Na_2S_2O_8{\cdot}5H_2O$), and hydrogen peroxide (H_2O_2) were obtained from Acros (Geel, Belgium). NaCN, NaSCN, CH_3COONa, $Na_2B_4O_7$, NaBr, $NaBrO_3$, NaCl, $NaClO_4$, Na_2CO_3, $Na_2C_2O_4$, NaF, NaI, $NaIO_3$, $NaNO_3$, Na_3PO_4, Na_2S, and Na_2SO_4 were obtained from Alfa Aesar (Ward Hill, MA). The pH value of the 100 mM phosphate solution (pH 10) was adjusted by mixing different volume ratios of H_3PO_4 (100 mM) and Na_3PO_4 (100 mM). Milli-Q ultrapure water was used in each experiment.

Preparation of FITC–BSA–Au NPs. We prepared 15 nM Au NPs (diameter: 13.3 nm ±0.5 nm) according to the previous report.[55] FITC-conjugated BSA (FITC–BSA) solution was prepared by the sequential addition of 700 μL deionized (DI) water, 100 μL phosphate buffer (50 mM, pH 10), 100 μL FITC (1.0 mM), and 100 μL BSA (100 μM) into a 1.5 mL vial. The resulting mixture was equilibrated at 4 °C for 6 h. After measurement of the fluorescence intensity at 520 nm (excitation at 480 nm; Synergy 4 Multi-Mode Microplate Reader, Biotek Instruments, Winooski, VT) for the unconjugated FITC that was separated by centrifugal filtration with a cutoff of 3 k at RCF 14 000*g* for 20 min. From the fluorescence measurement results, we estimated that there were 3.6 FITC molecules per BSA molecule. An aliquot of the unpurified FITC-conjugated BSA solution (900 μL) was added to a solution of the 13 nm Au NPs (11.1 nM, 8.1 mL) in 5 mM sodium phosphate (pH 10) and incubated at ambient temperature for 1 h. Prior to use, the excess FITC–BSA or FITC in the solution was removed by centrifugation (RCF 24 000*g*) for 20 min. After discarding the supernatant, the oily precipitate was washed with 5 mM sodium phosphate (pH 10). After three wash–centrifuge cycles, the FITC–BSA–Au NPs were resuspended separately in 5 mM sodium phosphate (pH 10) and stored in a refrigerator (4 °C). After measuring the fluorescence intensities of the supernatant FITC–BSA and FITC, they were further separated by centrifugal filtration (3 k) and we estimated that there were 415 FITC and 18 FITC–BSA molecules per Au NP. The fluorescence spectrum of the purified FITC–BSA–Au NP solution (excitation at 480 nm) revealed very

dx.doi.org/10.1021/am3003044 | ACS Appl. Mater. Interfaces 2012, 4, 2652–2658

weak fluorescence, suggesting that the solution contained a negligible amount of free FITC or FITC–BSA. It is worth noting that, the purified FITC–BSA–Au NP sample was stable for at least 6 months when stored at 4 °C in the dark.

Detection of Iodide and Cyanide Anions. A series of mixtures (0.5 mL) of anions (0–10 μM) and FITC–BSA–Au NPs (0.5 nM) in buffer solution (5 mM sodium phosphate; pH 10) was equilibrated at room temperature for 1 h and then transferred separately to 96-well microtiter plates. Their fluorescence spectra were recorded by a Synergy 4 Multi-Mode Microplate Reader. For the selective determination of I^- and CN^- anions, we equilibrated masking agents with the anion solutions for 10 min prior to the addition of FITC–BSA–Au NP probes. Herein, we only provide the final concentrations of the species.

Analysis of Real Samples. Seawater and pond water samples were collected from the East China Sea and the National Taiwan Ocean University campus, respectively; local tap water was filtered through a 0.2-μm membrane and used. Aliquots of the water samples (250 μL) were spiked with standard solutions of I^- or CN^- at the desired concentrations. Then, we diluted the spiked samples to 500 μL using a solution containing the FITC–BSA–Au NPs (0.5 nM) and 5 mM sodium phosphate (pH 10). The fluorescence spectra of spiked samples were recorded by a Synergy 4 Multi-Mode Microplate Reader.

Three edible salts with different KIO_3 levels were purchased from Taiwan Salt Industrial Corporation (Miaoli, Taiwan). Prior to analysis, an edible salt (0.3 g) was dissolved in 1 mL of DI water. The salt solution was then treated for 10 min with 5.0 mM ascorbic acid to reduce IO_3^- to I^-. The resulting solutions were spiked with a standard solution of I^- anions at desired concentrations and they were finally diluted with a solution containing 0.5 nM FITC–BSA–Au NPs and 5 mM sodium phosphate (pH 10). The spiked samples were also analyzed by inductively coupled plasma mass spectrometry (ICP-MS).

RESULTS AND DISCUSSION

Preparation of FITC–BSA–Au NPs. We prepared FITC–BSA–Au NPs using a facile strategy, merely by mixing FITC–BSA-conjugated solution with Au NPs. The free FITC and FITC–BSA were self-adsorbed on Au NP surfaces via physical interactions (Scheme 1). In their unbound state, FITC molecules are highly fluorescent (quantum yield >94%); however, when they are in close proximity to the Au NPs, the fluorescence of dye molecules is quenched efficiently through energy transfer and electron transfer processes. The inner filter effect (IFE) of Au NPs also contributes to the fluorescence quenching of FITC.[56] The main reasons for our choice of FITC as the dye in this study are its water solubility, high extinction coefficient, high quantum yield, and its fluorescence emission profile, which was significantly overlapped by the absorption band of Au NPs (quenching constant, K_{sv}, with Au NPs ≈ 4.8×10^{-10} M^{-1}).[57] A combination of electrostatic attraction, π–π interaction, and Au–S interaction between the citrate-capped Au NPs and the dye molecules controlled the interaction between Au NPs and FITC molecules.[57] From the fluorescence intensities of the supernatants of free FITC and FITC–BSA, we estimated that the amounts of FITC and FITC–BSA absorbed on each Au NP were 415 FITC and 18 FITC–BSA molecules, respectively. Au NPs exhibit high tolerance toward the salinity of aqueous solutions after being capped with BSA, which appears to bind spontaneously to the surfaces of negatively charged Au NPs predominantly via electrostatic mechanism, although we cann't neglect the contribution from hydrophobic interactions with the surface layer.[58,59] From dynamic light scattering (DLS) measurements, we estimated that the hydrodynamic diameters of the unlabeled Au NPs and FITC–BSA–Au NP assemblies were 18.3 (±6.2) and 35.2 (± 7.5) nm, respectively. The as-prepared FITC–BSA–Au NP retained their stability (no aggregation) in 5 mM sodium phosphate (pH 10) solution containing up to 100 mM NaCl (Figure S1 in the Supporting Information). In addition, the FITC–BSA–Au NPs could be stored in the lyophilized solid form. The isoelectric point (*p*I) of BSA is 4.6 and therefore the BSA has negative net charge in 5 mM sodium phosphate (pH 10). Regardless of the overall charge, BSA has 60 surface lysine groups that can have electrostatic interactions with negatively charged moieties. Thus, the adsorption of BSA to Au NPs is established through electrostatic interaction between the anionic groups ($-COO^-$) on the nanoparticles and the positively charged amino groups ($-NH_3^+$) of the lysine residues of the BSA.[59] Apart from the electrostatic interaction, ionic/hydrogen bonding between $-NH_3^+$ and $-COO^-$ caped surface is also feasible. The high stability of FITC–BSA–capped Au NPs were mainly because of the steric repulsive force (bulky proteins on the surface prevented neighboring Au NPs from attaining the close proximity needed to interact and aggregate), electrostatic repulsion, and high hydrophilicity of BSA.[59]

Sensing S^{2-}, CN^-, and I^- Using FITC–BSA–Au NP Probe. As indicated in Scheme 1, the sensing mechanisms occur via two routes: (i) anions displacing FITC dye molecules from the surfaces of Au NPs by the deposition of CN^-, S^{2-}, or I^- on the particles, and (ii) CN^--induced leaching of Au NPs. As a result, the fluorescence of FITC and FITC–BSA were restored. To detect CN^-, S^{2-}, or I^- ions, we performed proof-of-concept experiments using the FITC–BSA–Au NPs (0.5 nM) in 5 mM sodium phosphate (pH 10). At pH 10, the I^- (p*K*a = −11), CN^- (pK_a = 9.3), and HS^-/S^{2-} (pKa_1 = 7.0; pK_{a_2} = 9.5–11.5) forms will be predominantly existing in solution. In highly basic media (pH > 10), these anions are easily converted to their oxidized forms. At pH 10, all of these anions were stable and had strong affinities for the FITC–BSA–Au NPs through strong interactions of Au^+–CN^- (K_f ($Au(CN)_2^-$) = 2×10^{38}), Au^+–I^- (K_f ($Au(I)_2^-$) = 5×10^{30}), and Au^+–S^{2-} (K_f (AuS^-) = 4×10^{35}), leading to significant increases in the fluorescence (Figure 1).[60–64] We also noted that at pH >10, a passive layer of $Au(OH)_3$ or Au_2O_3 may form on the surface of the Au NPs.[65]

We used X-ray photoelectron spectroscopy (XPS) to investigate the oxidation states of the surfaces of the Au NPs (5 nM) in the absence and presence of CN^- (10 μM), I^- (10 μM), or S^{2-} (10 μM). The binding energy (BE) for the Au $4f_{7/2}$ electrons in the FITC–BSA–Au NPs in the absence of these anions was 83.7 eV (Figure S2, curve a in the Supporting Information), which is presumably within the range from 83.5 (Au) to 85.0 eV [polynuclear Au(I)–ligand complex].[66,67] The BEs of the Au NPs in the presence of CN^-, I^-, and S^{2-} were 84.7, 83.8, and 83.9 eV, respectively (Figure S2, curves b–d in the Supporting Information). The higher BE was primarily due to the greater contribution of these anion-passivated surfaces (i.e., the higher-BE component of Au^+) to the Au_{4f} core-level photoemission spectrum. The much higher BE of Au NP in the presence of CN^- indicates that some Au NPs were dissolved as $Au(CN)_2^-$ in solution. From surface-assisted laser desorption/ionization time-of-flight mass spectrometry (SALDI-TOF-MS) measurements, the signals of $[Au(CN)_2]^-$, $[Au_2(CN)]^-$, $[AuI_2]^-$, and $[AuS_2]^-$ reveal that these anions interact strongly with Au^+ on the particle surfaces (Figure S3 in the Supporting Information). The Raman vibrational signals observed at 2154, 156, and 453 cm^{-1} for CN^-, I^-, and S^{2-}, respectively, in the

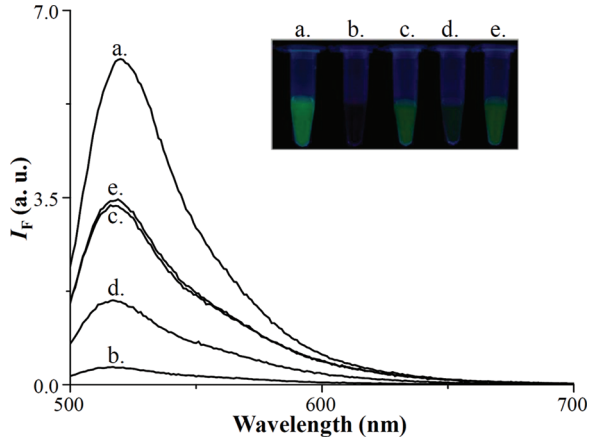

Figure 1. Fluorescence spectra of solutions of (a) FITC (207.5 nM)/FITC–BSA (9 nM), (b) FITC–BSA–Au NPs (0.5 nM), (c) FITC–BSA–Au NPs (0.5 nM) and NaCN (10 μM), (d) FITC–BSA–Au NPs (0.5 nM) and KI (10 μM), and (e) FITC–BSA–Au NPs (0.5 nM) and Na_2S (10 μM). Inset: Fluorescence photographs of the solutions on excitation under a hand-held UV lamp (365 nm). Buffer: 5 mM sodium phosphate, pH 10. Excitation wavelength: 480 nm. Fluorescence intensities (I_F) are plotted in arbitrary units (a. u.).

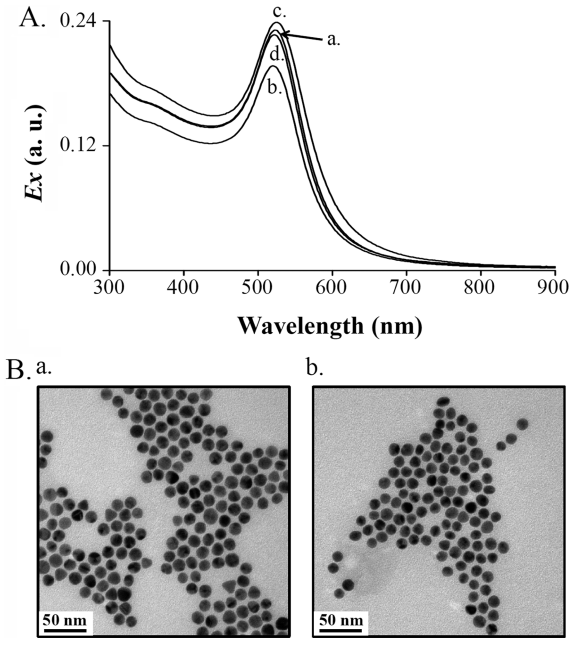

Figure 2. (A) UV–vis absorption spectra of 5 mM sodium phosphate (pH 10) solutions containing (a) FITC–BSA–Au NPs (0.5 nM), (b) FITC–BSA–Au NPs (0.5 nM) and NaCN (10 μM), (c) FITC–BSA–Au NPs (0.5 nM) and KI (10 μM), and (d) FITC–BSA–Au NPs (0.5 nM) and Na_2S (10 μM). (B) TEM images of (a) FITC–BSA–Au NPs and (b) FITC–BSA–Au NPs in the presence NaCN. Other conditions were the same as those described in Figure 1. Average particle sizes in B for (a) FITC–BSA–Au NPs and (b) FITC–BSA–Au NPs reacted with NaCN were 13.3 ± 0.5 nm and 10.0 ± 0.2 nm, respectively.

presence of Au NPs further demonstrated that these anions were deposited on the Au NP surfaces (see Figure S4 in the Supporting Information).

The fluorescence enhancements ($(I_F - I_{F0})/I_{F0}$), where I_F and I_{F0} represent the fluorescence intensities of FITC–BSA–Au NPs at 520 nm in the presence and absence of anions, respectively (Figure 1), followed the order S^{2-} (10.8) ≈ CN^- (10.4) > I^- (4.9). This trend was probably due to the fact that S^{2-} and CN^- form the most stable complexes (higher formation constants) with Au^+ on the particle's surface; as a result, more FITC molecules departed from the Au NP surfaces, and thereby restored the higher fluorescence signal of FITC in the presence of S^{2-} or CN^-. Compared with I^- and S^{2-}, the SPR band of FITC–BSA–Au NPs decreased after reacting with CN^-, indicating the dissolution of Au NPs (Figure 2A). The TEM images reveal that the particle sizes of FITC–BSA–Au NPs (0.5 nM) in the absence and presence of CN^- (10 μM) were 13.3 ± 0.5 nm and 10.0 ± 0.2 nm, respectively (Figure 2B). There was no statistical difference in the average particle diameter or size distribution of Au NPs in the absence and presence of S^{2-} or I^- as determined from TEM images (data not shown), revealing that there is only a monolayer or submonolayer of S^{2-} or I^- on the surface of Au NPs. The dissolution of Au NPs by CN^-, which leads to the decrease in the IFE, also contributed to the restoration of stronger fluorescence signal of FITC. In a control experiment, we observed that none of the ions—CN^-, S^{2-}, or I^-—in the concentration range 100 nM–10 μM caused changes in the fluorescence intensity of 100 nM FITC or 10 nM FITC–BSA solutions (data not shown).

Selectivity and Sensitivity. To evaluate the selectivity of the proposed fluorimetric assay, we determined the values of $(I_F - I_{F0})/I_{F0}$ for the FITC–BSA–Au NP probe (0.5 nM) in the presence of different anions (10 μM). Figure 3A reveals that the addition of CN^-, I^-, and S^{2-} to solutions of FITC–BSA–Au NPs resulted in an apparent restoration of the fluorescence, whereas the other remaining anions had insignificant effects under the same experimental conditions. H_2O_2 possesses a strong oxidation ability (E^0 = −0.695 V) for CN^- ($CN^- + H_2O_2 \rightarrow CNO^- + H_2O$; $K = 4.9 \times 10^{75}$) and S^{2-} ($S^{2-} + 4H_2O_2 \rightarrow SO_4^{2-} + 4H_2O$; $K = 9.8 \times 10^{46}$) under alkaline pH conditions.[68,69] Therefore, the use of H_2O_2 (100 mM) as a masking agent greatly suppressed the interference from the CN^- and S^{2-} anions, allowing the FITC–BSA–Au NP sensor to exhibit excellent selectivity for I^- (see Figure 3B). The FITC–BSA–Au NPs (0.5 nM) in 5 mM sodium phosphate buffer (pH 10) containing H_2O_2 (100 mM) exhibited a selectivity of 250-fold for I^- over other metal ions. Under optimal conditions, we quantified the I^- levels by monitoring the fluorescence enhancement ($(I_F - I_{F0})/I_{F0}$) of the solution of FITC–BSA–Au NPs (0.5 nM) containing H_2O_2 (100 mM). When the I^- ion concentration was increased, we observed a gradual increase in the fluorescence intensity of the probe solution (Figure 4). The plots of relative fluorescence $(I_F - I_{F0})/I_{F0}$ at 520 nm exhibited a good linearity over the I-concentrations ranging from 1 to 1000 nM with a correlation coefficient (R) of 0.98. This method enabled the selective sensing of I^- with a limit of detection (LOD) of 50 nM with a signal-to-noise (S/N) ratio of 3. Although the sensitivity of this FITC–BSA–Au NP sensor is one to 2 orders of magnitude less than those of other analytical methods (e.g., ICP-MS), its low cost, ease of use, and lack of sample pretreatment suggest that it can be potentially applied to the selective detection of I^- in real samples.

Next, we investigated the effects of the masking agents such as—$S_2O_8^{2-}$ and Pb^{2+} and their mixtures—on the FITC–BSA–Au NP sensing system. To our delight, our nanosensor was specific for CN^- with respect to the other metal ion species in the presence of 20 mM $Na_2S_2O_8$ and 10 μM $Pb(NO_3)_2$ (see

dx.doi.org/10.1021/am3003044 | ACS Appl. Mater. Interfaces 2012, 4, 2652–2658

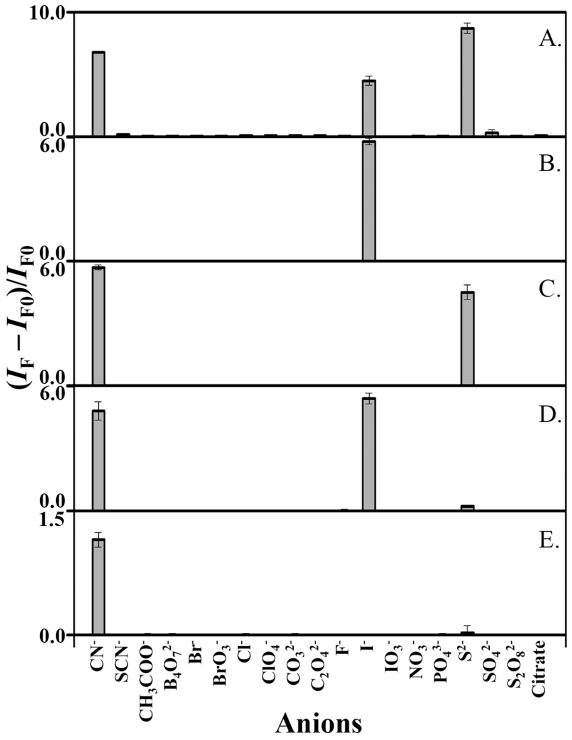

Figure 3. (A) Selectivities of FITC–BSA–Au NP (0.5 nM) sensor for different anions (10 μM) in the (A) absence of a masking reagent and in the (B–E) presence of (B) H_2O_2 (100 mM), (C) $K_2S_2O_8$ (20 mM), (D) $Pb(NO_3)_2$ (10 μM), and (E) $K_2S_2O_8$ (20 mM) and $Pb(NO_3)_2$ (10 μM). Error bars represent the standard deviations from five repeated experiments. Other conditions were the same as those described in Figure 1.

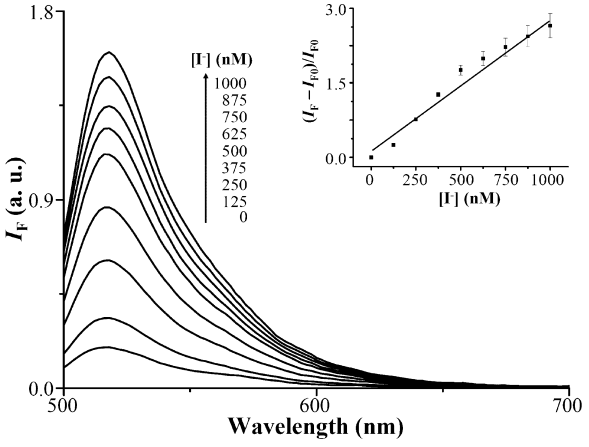

Figure 4. Fluorescence spectra of the FITC–BSA–Au NP (0.5 nM) solutions used as probes for the detection of I^- (0–1.0 μM) in the presence of H_2O_2 (100 mM) in 5 mM sodium phosphate (pH 10). Inset: Plot of relative fluorescence $(I_F - I_{F0})/I_{F0}$ versus I^- ion concentration. Other conditions were the same as those described in Figure 3B.

Figure 3E). The oxidation of I^- to molecular iodine (I_2) using $Na_2S_2O_8$ ($S_2O_8^{2-} + 2\ I^- \rightarrow 2\ SO_4^{2-} + I_2$; $K = 7 \times 10^{15}$) can mask the I^- ions.[70] To improve the selectivity of the FITC–BSA–Au NPs for CN^-, we used Pb^{2+} as a second masking agent to take advantage of the stronger formation constant of PbS ($\log K_f \sim 28$), whereas the $\log K_f$ values of $Pb(CN)_4^{2-}$ and PbI_4^{2-} were 2.2×10^8 and 1.6×10^6, respectively.[71−73] As indicated in Figure 3E, FITC–BSA–Au NPs (0.6 nM) in 5 mM sodium phosphate (pH 10) containing the masking agents (20 mM $Na_2S_2O_8$ and 10 μM $Pb(NO_3)_2$) demonstrated high selectivity for CN^- ions with respect to the other metal ions (>150-fold) at the same concentration. The fluorescence intensity of the FITC–BSA–Au NPs (0.5 nM) in 5 mM sodium phosphate (pH 10) containing the masking agents (20 mM $Na_2S_2O_8$ and 10 μM $Pb(NO_3)_2$) gradually increased with the CN^- ion concentration (Figure 5). A linear correlation (R =

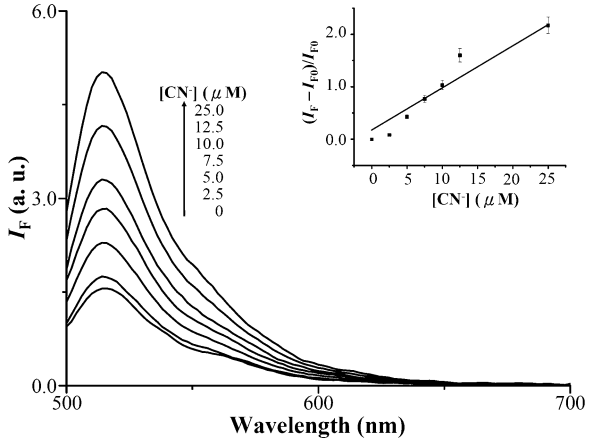

Figure 5. Fluorescence spectra of the FITC–BSA–Au NP (0.5 nM) solutions used as probes for the detection of CN^- (0–25 μM) in the presence of 20 mM $Na_2S_2O_8$ and 10 μM $Pb(NO_3)_2$ in 5 mM sodium phosphate (pH 10). Inset: Plot of relative fluorescence $(I_F - I_{F0})/I_{F0}$ versus CN^- ion concentration. Other conditions were the same as those described in Figure 3E.

0.97) existed between the value of relative fluorescence $(I_F - I_{F0})/I_{F0}$ and the concentration in the range 0–10 μM. The LOD of CN^- was 1.0 μM with a S/N ratio of 3. To the best of our knowledge, our system utilizes the first, label-free, Au-NP-based optical sensors for the selective detection of I^- and CN^- ions with different masking agents. Compared with the above-mentioned methods, the advantages of this FITC–BSA–Au NP probe include low cost, easy preparation, and high salt resistance. Our results suggested that this FITC–BSA–Au NP probe would be sensitive for monitoring the I^- and CN^- ions levels in environmental samples.

Analysis of CN^- and I^- in Real Samples. To validate the practicality of our proposed sensing strategy for the analysis of CN^- and I^- in environmental samples, we used the FITC–BSA–Au NP sensor to determine the levels of CN^- and I^- in pond water, seawater–water, and tap water. We obtained similar linear correlations (R = 0.95–0.99) between the response and the CN^- and I^- ion concentrations spiked into the three different water samples (diluted 10-fold) over the ranges 0–10 μM and 0 nM–1.0 μM, respectively (see Figure S5 in the Supporting Information). In these measurements, the $S_2O_8^{2-}/Pb^{2+}$-FITC–BSA–Au NP and H_2O_2–FITC–BSA–Au NP probes provided recoveries of 95–108% and 96–104% for CN^- and I^- ions, respectively. The minimum detectable concentration of CN^- and I^- ions by our $S_2O_8^{2-}/Pb^{2+}$–FITC–BSA–Au NP and H_2O_2–FITC–BSA–Au NP probes in these water samples was approximately 1000 nM and 50 nM, respectively. Note that the detection limit of our $S_2O_8^{2-}/Pb^{2+}$–FITC–BSA-Au NPs in these water samples was much lower than the MAL of CN^- (200 ppb) in drinking water set by the U.S. EPA.

dx.doi.org/10.1021/am3003044 | ACS Appl. Mater. Interfaces 2012, 4, 2652–2658

Table 1. Determination of I^- Concentrations in Edible Salt Samples by H_2O_2–FITC–BSA–Au NP Probes

salt sample	certified range (ppm)	ICP-MS value, mean ± SD (μM, n = 5)	H_2O_2–FITC–BSA–Au NP probes, mean ± SD (ppm, n = 5)	spiked [I^-] (nM)	R	t-test between ICP-MS and H_2O_2–FITC–BSA–Au NP probes[a]	consensus value (μM), 95% confidence interval[a]
sample A	0	0.8 ± 0.1	0.6 ± 0.1	0–700	0.94	2.36	0.5–0.7
sample B	15.2	15.9 ± 0.5	16.4 ± 0.5	0–700	0.98	2.58	15.2–17.6
sample C	35.5	36.5 ± 1.5	37.2 ± 1.2	0–700	0.98	2.12	33.4–41.0

[a] T-test value is 2.77 at a 95% confidence level (n = 5).

We also utilized our sensor system to determine the iodide concentrations in edible salt samples because iodized salt is used to help reduce the incidence of iodine deficiency in humans.[74] The iodide content in iodized salt is recommended to be 46–77 ppm and 10–22 ppm in the United States and the United Kingdom, respectively.[75,76] The major component of the iodine species in our purchased edible salt is IO_3^-. We pretreated the salt with 5 mM ascorbic acid to reduce it to $I^-$and determined the concentration of iodide ions in the three edible salt samples by applying a standard addition method (see Figure S6 in the Supporting Information). Using a t-test, we found that the 95% confidence intervals for the iodide ions were in good agreement with the certified values and ICP-MS measurements (Table 1). In addition, the FITC–BSA–Au NP probe could be used to easily screen the iodide level in edible salt samples with the naked eye (see Figure S7 in the Supporting Information).

CONCLUSIONS

We developed two fluorescent nanosensors, both featuring FITC–BSA-capped Au NPs, for the selective and sensitive sensing of CN^- and I^- ions in high-salinity solutions. The FITC–BSA–Au NPs were stable in solutions containing up to 100 mM NaCl. In the presence of the masking agents $S_2O_8^{2-}$/Pb^{2+}, FITC–BSA–Au NPs permitted the detection of CN^- with selectivity (no less than 150-fold upon comparing with other anions). The sensitivity of our assay for the detection of CN^- levels in water samples (tap, pond, and seawater) is much higher than the standard limit by the U.S. EPA. We also demonstrated that H_2O_2–FITC–BSA–Au NPs could selectively detect I^- down to 50 nM. Taking advantage of their high stability and selectivity, we applied our H_2O_2–FITC–BSA–Au NPs for the detection of I^- in real water and edible salt samples. The results of the I^- determination in three edible salt samples by our H_2O_2–FITC–BSA–Au NP probes are in good agreement with those obtained using ICP-MS. In comparison with other Au-NP-based optical methods for the detection of anions, our FITC–BSA–Au NPs showed good salt tolerance and selectivity with suitable masking agents. The FITC–BSA–Au NP probes should eliminate the need for synthesis of complicated chemosensors or the use of sophisticated equipment. This simple, rapid, and cost-effective sensing system appears to hold great practical potential for the detection of anions in real samples.

ASSOCIATED CONTENT

Supporting Information

Additional information, as noted in the text. This material is available free of charge via the Internet at http://pubs.acs.org.

AUTHOR INFORMATION

Corresponding Author

*Tel.: 011-886-2-2462-2192, ext 5517 (C.-C.H.); 011-886-4-7232-105, ext 3522 (Y.-W.L.). Fax: 011-886-2-2462-2320 (C.-C.H.). E-mail: huanging@ntou.edu.tw (C.-C.H.); linywjerry@cc.ncue.edu.tw (Y.-W.L.).

Notes

The authors declare no competing financial interest.

ACKNOWLEDGMENTS

This study was supported by the National Science Council of Taiwan under Contract 99-2113-M-019-001-MY2.

REFERENCES

(1) Pissuwan, D.; Niidome, T.; Cortie, M. B. *J. Controlled Release* **2011**, *149*, 65–71.
(2) Syed, M. A.; Bokhari, S. H. *J. Biomed. Nanotechnol.* **2011**, *7*, 229–237.
(3) Alexandridis, P. *Chem. Eng. Technol.* **2011**, *34*, 15–28.
(4) Xu, X.; Daniel, W. L.; Wei, W.; Mirkin, C. A. *Small* **2010**, *6*, 623–626.
(5) Krpetić, Ž.; Saleemi, S.; Prior, I. A.; Sée, V.; Qureshi, R.; Brust, M. *ACS Nano* **2011**, *5*, 5195–5201.
(6) Xia, F.; Zuo, X.; Yang, R.; Xiao, Y.; Kang, D.; Vallée-Bélisle, A.; Gong, X.; Yuen, J. D.; Hsu, B. B. Y.; Heeger, A. J.; Plaxco, K. W. *Proc. Natl. Acad. Sci. U.S.A.* **2010**, *107*, 10837–10841.
(7) Knecht, M. R.; Sethi, M. *Anal. Bioanal. Chem.* **2009**, *394*, 33–46.
(8) Lee, J. H.; Yigit, M. V.; Mazumdar, D.; Lu, Y. *Adv. Drug Delivery Rev.* **2010**, *62*, 592–605.
(9) Cao, X.; Ye, Y.; Liu, S. *Anal. Biochem.* **2011**, *417*, 1–16.
(10) Jiao, P. F.; Zhou, H. Y.; Chen, L. X.; Yan, B. *Curr. Med. Chem.* **2011**, *18*, 2086–2102.
(11) Kumar, S. A.; Khan, M. I. *Curr. Med. Chem.* **2010**, *10*, 4124–4134.
(12) Li, B.; Dong, S.; Wang, E. *Chem. Asian J.* **2010**, *5*, 1262–1272.
(13) Rokita, S. E.; Adler, J. M.; McTamney, P. M.; Watson, J. A., Jr. *Biochimie* **2010**, *92*, 1227–1235.
(14) Hingorani, M.; Spitzweg, C.; Vassaux, G.; Newbold, K.; Melcher, A.; Pandha, H.; Vile, R.; Harrington, K. *Curr. Cancer Drug Targets* **2010**, *10*, 242–267.
(15) Pearce, E. N. *Arch. Intern. Med.* **2012**, *172*, 159–161.
(16) Küpper, F. C.; Feiters, M. C.; Olofsson, B.; Kaiho, T.; Yanagida, S.; Zimmermann, M. B.; Carpenter, L. J.; Luther, G. W., III; Lu, Z.; Jonsson, M.; Kloo, L. *Angew. Chem., Int. Ed.* **2011**, *50*, 11598–11620.
(17) Kulig, K. W.; Ballantyne, B.; Becker, C.; Borak, J.; Cannella, J.; Goldstein, B.; Hall, A.; Jackson, R. J.; Rodnick, J.; Wheater, R.; Wummer, B. *Am. Fam. Physician* **1993**, *48*, 107–109.
(18) Nůsková, H.; Vrbacký, M.; Drahota, Z.; Houštěk, J. *J. Bioenergy Biomembr.* **2010**, *42*, 395–403.
(19) Borron, S. W.; Baud, F. J. *Arh. Hig. Rada Toksikol.* **1996**, *47*, 307–322.
(20) Yeoh, M. J.; Braitberg, G. *J. Toxicol. Clin. Toxicol.* **2004**, *42*, 855–863.
(21) *EPA 816-F-09-0004: Safe Drinking Water 2009*; U.S. Environmental Protection Agency: Washington, D.C., 2009.
(22) Mottier, N.; Jeanneret, F.; Rotach, M. *J. AOAC Int.* **2010**, *93*, 1032–1038.

(23) Minakata, K.; Yamagishi, I.; Kanno, S.; Nozawa, H.; Suzuki, M.; Suzuki, O. *J. Chromatogr. B* **2010**, *878*, 1683−1686.
(24) Chena, Z.; Megharaj, M.; Naidu, R. *Talanta* **2007**, *72*, 1842−1846.
(25) Pantůč ková, P.; Urbánek, M.; Křivánková, L. *Electrophoresis* **2007**, *28*, 3777−3785.
(26) Jermak, S.; Pranaitytė, B.; Padarauskas, A. *J. Chromatogr. A* **2007**, *1148*, 123−127.
(27) Minakata, K.; Nozawa, H.; Gonmori, K.; Yamagishi, I.; Suzuki, M.; Hasegawa, K.; Watanabe, K.; Suzuki, O. *Anal. Bioanal. Chem.* **2011**, *400*, 1945−1951.
(28) Zeng, Q.; Cai, P.; Li, Z.; Qin, J.; Tang, B. Z. *Chem. Commun.* **2008**, 1094−1096.
(29) Ma, B.; Zeng, F.; Zheng, F.; Wu, S. *Chem.—Eur. J.* **2011**, *17*, 14844−14850.
(30) Rastegarzadeh, S.; Pourreza, N.; Saeedi, I. *Talanta* **2009**, *77*, 1032−1036.
(31) Lee, D. Y.; Singh, N.; Satyender, A.; Jang, D. O. *Tetrahedron Lett.* **2011**, *52*, 6919−6922.
(32) Chen, X.; Nam, S.-W.; Kim, G.-H.; Song, N.; Jeong, Y.; Shin, I.; Kim, S. K.; Kim, J.; Park, S.; Yoon, J. *Chem. Commun.* **2010**, *46*, 8953−8955.
(33) Park, I. S.; Heo, E.-J.; Kim, J.-M. *Tetrahedron Lett.* **2011**, *52*, 2454−2457.
(34) Zelder, F. H. *Inorg. Chem.* **2008**, *47*, 1264−1266.
(35) Lou, X.; Zeng, Q.; Zhang, Y.; Wan, Z.; Qin, J.; Li, Z. *J. Mater. Chem.* **2012**, *22*, 5581−5586.
(36) Chen, Y.-M.; Cheng, T.-L.; Tseng, W.-L. *Analyst* **2009**, *134*, 2106−2112.
(37) Jung, E.; Kim, S.; Kim, Y.; Seo, S. H.; Lee, S. S.; Han, M. S.; Lee, S. *Angew. Chem., Int. Ed.* **2011**, *50*, 4386−4389.
(38) Zhang, J.; Xu, X.; Yang, C.; Yang, F.; Yang, X. *Anal. Chem.* **2011**, *83*, 3911−3917.
(39) Pienpinijtham, P.; Han, X. X.; Ekgasit, S.; Ozaki, Y. *Anal. Chem.* **2011**, *83*, 3655−3662.
(40) Lou, X.; Zhang, Y.; Qin, J.; Li, Z. *Chem.—Eur. J.* **2011**, *17*, 9691−9696.
(41) Senapati, D.; Dasary, S. S. R.; Singh, A. K.; Senapati, T.; Yu, H.; Ray, P. C. *Chem.—Eur. J.* **2011**, *17*, 8445−8451.
(42) Shang, L.; Dong, S. *Anal. Chem.* **2009**, *81*, 1465−1470.
(43) Liu, C.-Y.; Tseng, W.-L. *Chem. Commun.* **2011**, *47*, 2550−2552.
(44) Zhai, Y.; Jin, L.; Wang, P.; Dong, S. *Chem. Commun.* **2011**, *47*, 8268−8270.
(45) Hajizadeh, S.; Farhadi, K.; Forough, M.; Sabzi, R. E. *Anal. Methods* **2011**, *3*, 2599−2603.
(46) Liu, Y.; Ai, K.; Cheng, X.; Huo, L.; Lu, L. *Adv. Funct. Mater.* **2010**, *20*, 951−956.
(47) Chen, W.-Y.; Lan, G.-Y.; Chang, H.-T. *Anal. Chem.* **2011**, *83*, 9450−9455.
(48) Della Gaspera, E.; Guglielmi, M.; Agnoli, S.; Granozzi, G.; Post, M. L.; Bello, V.; Mattei, G.; Martucci, A. *Chem. Mater.* **2010**, *22*, 3407−3417.
(49) Lee, J.; Mubeen, S.; Hangarter, C. M.; Mulchandani, A.; Chen, W.; Myung, N. V. *Electroanal.* **2011**, *23*, 2623−2628.
(50) Mubeen, S.; Zhang, T.; Chartuprayoon, N.; Rheem, Y.; Mulchandani, A.; Myung, N. V.; Deshusses, M. A. *Anal. Chem.* **2010**, *82*, 250−257.
(51) Zhang, J.; Xu, X.; Yuan, Y.; Yang, C.; Yang, X. *ACS Appl. Mater. Interfaces* **2011**, *3*, 2928−2931.
(52) Daniel, W. L.; Han, M. S.; Lee, J.-S.; Mirkin, C. A. *J. Am. Chem. Soc.* **2009**, *131*, 6362−6363.
(53) Massue, J.; Quinn, S. J.; Gunnlaugsson, T. *J. Am. Chem. Soc.* **2008**, *130*, 6900−6901.
(54) (a) Zhang, J.; Yuan, Y.; Xu, X.; Wang, X.; Yang, X. *ACS Appl. Mater. Inter.* **2011**, *3*, 4092−4100. (b) Tripathy, S. K.; Woo, J. Y.; Han, C.-S. *Anal. Chem.* **2011**, *83*, 9206−9212.
(55) Turkevich, J.; Stevenson, P. C.; Hillier, J. *Faraday Discuss.* **1951**, *11*, 55−75.
(56) Shang, L.; Qin, C.; Jin, L.; Wang, L.; Dong, S. *Analyst* **2009**, *134*, 1477−1482.
(57) Sironi, L.; Freddi, S.; D'Alfonso, L.; Collini, M.; Gorletta, T.; Soddu, S.; Chirico, G. *J. Biomed. Nanotechnol.* **2009**, *5*, 683−691.
(58) Chang, H.-Y.; Hsiung, T.-M.; Huang, Y.-F.; Huang, C.-C. *Environ. Sci. Technol.* **2011**, *45*, 1534−1539.
(59) Brewer, S. H.; Glomm, W. R.; Johnson, M. C.; Knag, M. K.; Franzen, S. *Langmuir* **2005**, *21*, 9303−9307.
(60) Castillo-Ortega, M. M.; Santos-Sauceda, I.; Encinas, J. C.; Rodriguez-Felix, D. E.; del Castillo-Castro, T.; Rodriguez-Felix, F.; Valenzuela-García, J. L.; Quiroz-Castillo, L. S.; Herrera-Franco, P. J. *J. Mater. Sci.* **2011**, *46*, 7466−7474.
(61) Baghalha, M. *Hydrometallurgy* **2012**, *113−114*, 42−50.
(62) Azizi, A.; Petre, C. F.; Assima, G. P.; Larachi, F. *Hydrometallurgy* **2012**, *113−114*, 51−59.
(63) Liu, X.; Fang, Y.; Jiang, H.; Xiao, Y.; Li, L. *Adv. Mater. Res* **2012**, *343−344*, 43−55.
(64) Hameed, A.; Islam, N. U.; Shah, M. R.; Kanwal, S. *Chem. Commun.* **2011**, *47*, 11987−11989.
(65) Burke, L. D. *Gold Bull.* **2004**, *37*, 125−135.
(66) Mikhlin, Y.; Likhatski, M.; Tomashevich, Y.; Romanchenko, A.; Erenburg, S.; Trubina, S. *J. Electron. Spectrosc.* **2010**, *177*, 24−29.
(67) Della Gaspera, E.; Guglielmi, M.; Giallongo, G.; Agnoli, S.; Granozzi, G.; Quaglio, F.; Martucci, A. *Sens. Lett.* **2011**, *9*, 591−594.
(68) Yeddou, A. R.; Chergui, S.; Chergui, A.; Halet, F.; Hamza, A.; Nadjemi, B.; Ould-Dris, A.; Belkouch, J. *Miner. Eng.* **2011**, *24*, 788−793.
(69) Le Maux, P.; Simonneaux, G. *Chem. Commun.* **2011**, *47*, 6957−6959.
(70) Secco, F.; Celsi, S. *J. Chem. Soc. A* **1971**, 1092−1096.
(71) Mozafari, M.; Moztarzadeh, F. *J. Colloid Interface Sci.* **2010**, *351*, 442−448.
(72) Jana, S.; Thapa, R.; Maity, R.; Chattopadhyay, K. K. *Physica E* **2008**, *40*, 3121−3126.
(73) Ramadan, A. A.; Mandil, H.; Maktabi, M. *Asian J. Chem.* **2010**, *22*, 3260−3266.
(74) Zhang, W.; Liu, X.; Jia, X.; Han, Y.; Liu, X.; Xie, X.; Lu, J.; Duan, T.; Chen, H. *Chromatographia* **2010**, *72*, 1009−1012.
(75) Scientific Committee on Food. *Opinion of the Scientific Committee on Food on the Tolerable Upper Intake Level of Iodine*; SCF/CS/NUT/UPPLEV/26 ; European Commission: Brussels, Belgium, 2002; http://europa.eu.int/comm/food/fs/sc/scf/out146_en.pdf.
(76) WHO/UNICEF/ICCIDD. *Recommended Iodine Levels in Salt and Guidelines for Monitoring their Adequacy and Effectiveness*; WHO/NUT/96.13 ; World Health Organization: Geneva, Switzerland, 1996.